Neuro-Oncology
22(5), 639–651, 2020 | doi:10.1093/neuonc/noz226 | Advance Access date 3 December 2019

Anti–PD-L1 antibody direct activation of macrophages contributes to a radiation-induced abscopal response in glioblastoma

Chibawanye I. Ene, Shannon A. Kreuser, Miyeon Jung, Huajia Zhang, Sonali Arora, Kara White Moyes, Frank Szulzewsky, Jason Barber, Patrick J. Cimino, Hans-Georg Wirsching, Anoop Patel, Paul Kong, Timothy R. Woodiwiss, Sharon J. Durfy, A. McGarry Houghton, Robert H. Pierce, Ian F. Parney, Courtney A. Crane, and Eric C. Holland

Department of Neurological Surgery, University of Washington, Seattle, Washington (C.I.E., J.B., A.P., S.J.D., C.A.C., E.C.H.); Human Biology Division, Fred Hutchinson Cancer Research Center, Seattle, Washington (C.I.E., H.Z., S.A., F.S., P.J.C., H-G.W., A.P., T.R.W., A.M.H., E.C.H.); Ben Towne Center for Childhood Cancer Research, Seattle Children's Research Institute, Seattle, Washington (S.A.K., K.W.M., C.A.C.); Department of Neurological Surgery, Mayo Clinic, Rochester, Minnesota (M.J., I.F.P.); Department of Pathology, Division of Neuropathology, University of Washington School of Medicine, Seattle, Washington (P.J.C.); Experimental Histopathology, Fred Hutchinson Cancer Research Center, Seattle Washington (P.K., R.H.P.); Alvord Brain Tumor Center, University of Washington, Seattle, Washington (C.A.C., E.C.H.); Department of Neurology, University Hospital and University of Zurich, Zurich, Switzerland (H.-G.W.)

Corresponding Author: Eric Holland, MD, PhD, Senior VP and Director, Division of Human Biology, Translational Cancer Research, Fred Hutchinson Cancer Research Center, 1100 Fairview Ave N, C3-168, Seattle, WA 98109 (eholland@fhcrc.org).

Abstract

Background. Most glioblastomas recur near prior radiation treatment sites. Future clinical success will require achieving and optimizing an "abscopal effect," whereby unirradiated neoplastic cells outside treatment sites are recognized and attacked by the immune system. Radiation combined with anti–programmed cell death ligand 1 (PD-L1) demonstrated modest efficacy in phase II human glioblastoma clinical trials, but the mechanism and relevance of the abscopal effect during this response remain unknown.

Methods. We modified an immune-competent, genetically driven mouse glioma model (forced platelet derived growth factor [PDGF] expression + phosphatase and tensin homolog loss) where a portion of the tumor burden is irradiated (PDGF) and another unirradiated luciferase-expressing tumor (PDGF + luciferase) is used as a readout of the abscopal effect following systemic anti–PD-L1 immunotherapy. We assessed relevance of tumor neoepitope during the abscopal response by inducing expression of epidermal growth factor receptor variant III (EGFRvIII) (PDGF + EGFRvIII). Statistical tests were two-sided.

Results. Following radiation of one lesion, anti–PD-L1 immunotherapy enhanced the abscopal response to the unirradiated lesion. In PDGF-driven gliomas without tumor neoepitope (PDGF + luciferase, $n = 8$), the abscopal response occurred via anti–PD-L1 driven, extracellular signal-regulated kinase–mediated, bone marrow–derived macrophage phagocytosis of adjacent unirradiated tumor cells, with modest survival implications (median survival 41 days vs radiation alone 37.5 days, $P = 0.03$). In PDGF-driven gliomas with tumor neoepitope (PDGF + EGFRvIII, $n = 8$), anti–PD-L1 enhanced abscopal response was associated with macrophage and T-cell infiltration and increased survival benefit (median survival 36 days vs radiation alone 28 days, $P = 0.001$).

Conclusion. Our results indicate that anti–PD-L1 immunotherapy enhances a radiation- induced abscopal response via canonical T-cell activation and direct macrophage activation in glioblastoma.

Key Points

1. Radiation synergizes with anti–PD-L1 immunotherapy in glioblastoma.
2. Tumor neoepitope may enhance response to radiation and anti–PD-L1 immunotherapy.
3. Anti–PD-L1 antibody directly activates macrophage phagocytic activity independently of T cells.

Importance of the Study

A recent phase II clinical trial assessing the combination of radiation and anti–PD-L1 immunotherapy in glioblastoma showed a modest improvement in patient survival. The relevance of the abscopal response or impact of tumor neoepitope for susceptibility of glioblastoma to radiation and anti–PD-L1 immunotherapy remains unclear. We developed a representative glioblastoma mouse model based on the replication-competent avian sarcoma-leukosis virus (ASLV) long terminal repeat (LTR) with a splice acceptor/tumor virus A (RCAS/Tva) system that allows for real-time assessment of the abscopal response following radiation of adjacent non-luciferase-expressing glioblastoma. Glioblastoma with tumor neoepitope such as EGFRvIII is more susceptible to the abscopal response with significant macrophage and T-cell infiltration. In other glioblastoma without neoepitope expression, anti–PD-L1 antibodies enhance a radiation-induced abscopal response through direct activation of an antitumor and pro-inflammatory phenotype in macrophages. Our results indicate that radiation and anti–PD-L1 induced abscopal response in glioblastoma may contribute to the modest survival benefit seen in human clinical trials.

Glioblastoma is a highly aggressive intrinsic brain tumor that is diffusely infiltrative into the brain parenchyma.[1] Most recurrences following standard treatment (surgery, chemotherapy, radiation) are within 2 cm of the prior treatment location.[2] Therefore, it is likely that any significant improvement in survival for glioblastoma patients will require assistance from the immune system to kill resistant/residual tumor cells outside prior treatment regions (abscopal response). During the abscopal response, radiation of specific tumors activates a systemic immune response to unirradiated and distant tumor foci.[3] In humans and mice, this effect is potentiated by immune checkpoint inhibitors, resulting in an antitumor immunologic response outside the radiation field, even within the central nervous system.[4,5]

The clinical relevance of an abscopal effect on survival of patients with late stage non–small cell lung cancer was previously assessed in a phase II prospective randomized clinical trial.[6] Results demonstrated that following a combination of radiation and anti–cytotoxic T lymphocyte antigen 4 immunotherapy, unirradiated distant lesions regressed. This regression was associated with T-cell activation, resulting in a significant improvement in progression-free survival (PFS; median = 7.1 vs 3 mo, $P < 0.001$) and overall survival (OS; median 20.4 vs 3.5 mo, $P < 0.001$).[6] A phase II prospective clinical trial combining radiotherapy with anti–programmed cell death ligand 1 (PD-L1) immunotherapy (MEDI4736, durvalumab) in newly diagnosed unmethylated glioblastomas demonstrated some efficacy, with median OS of 15.1 months versus a historical median OS of 12.7 months for new unmethylated glioblastoma.[7] Although a phase III clinical trial is necessary to confirm these findings, it is suggested that the combination of radiation and anti–PD-L1 immunotherapy may enhance an immunologic response to glioblastoma. It remains unclear whether, similar to non–small cell lung cancer, the abscopal response contributes to this effect on survival. It is also unclear which tumor-specific factors, such as neoepitopes or peripheral immunosuppressive mechanisms, may influence susceptibility to this treatment combination. Further, it remains uncertain what strategies could optimize the abscopal phenomenon for glioblastoma following radiation and anti–PD-L1 therapy.

In the current study, we leverage the mouse model system of replication-competent avian sarcoma-leukosis virus long terminal repeat splice acceptor (RCAS)/tumor virus A (TVA) to study factors influencing susceptibility to the abscopal response in the setting of standard targeted radiation combined with anti–PD-L1 immunotherapy.

Materials and Methods

A detailed description of the methods can be found in the Supplementary Material (available online). All animal experiments were done in accordance with guidelines from the Institutional Animal Care and Use Committee at the Fred Hutchinson Cancer Research Center (IACUC protocol #50842).

Mouse Models of Glioblastoma

The RCAS/TVA model system was used to generate mouse glioblastoma.[8,9] The (1) Tg(*NTva*); *Cdkn2a (Ink4a-Arf)*$^{-/-}$; *Pten*$^{flox/flox}$ (referred to as *NTva*), Tg(*NTva*); *Cdkn2a (Ink4a-Arf)*$^{-/-}$; *Pten*^{floxlflox}; *LSL Luciferase* and EGFRvIII and (2) Tg(*NTva*); *Cdkn2a*^{wt}; *Pten*$^{flox/flox}$; *CX3CR1*$^{+/GFP}$; *CCR2*$^{+/RFP}$ mice[10] were used as genetic backgrounds for RCAS-mediated glioblastoma formation. Details of the full epidermal growth factor receptor variant III (EGFRvIII) cDNA, which also encodes the unique EGFRvIII splice junction peptide or neoepitope (peptide sequence LEEKKGNYVVTDH), and mice strains used for conditional overexpression were previously described[11,12] and summarized in the Supplementary Material online. For bilateral tumor models, following introduction of RCAS–platelet derived growth factor B (*PDGFB*) with RCAS-*Cre* into one hemisphere and RCAS-*PDGFB* with RCAS–short hairpin phosphatase and tensin homolog (*shPten*) into the contralateral hemisphere, 2 genetically similar tumors develop, with one tumor lacking luciferase expression (PDGFB/shPten; radiated glioblastoma) and the other tumor demonstrating luciferase or EGFRvIII expression (unirradiated glioblastoma).

Bilateral Tumor Formation In Vivo

Bilateral tumors were generated in 4- to 6-week-old male and female adult mice. DF1 cell delivery was performed with a 30-gauge needle attached to a Hamilton syringe and stereotactic fixation device (Stoelting). Cells were injected

into the frontal cortex of each hemisphere, 3 mm lateral to bregma and a depth of 1 mm. Mice were monitored carefully for signs of disease, and treatment began when the tumor was visible by bioluminescence or MRI.

Drug Treatments In Vivo

Adult mice were sedated with isoflurane during radiation. Ten grays was delivered to the right hemisphere (non-luciferase tumor), while the left hemisphere (luciferase- or EGFRvIII-expressing tumor) and the rest of body were shielded to prevent radiation on nontarget tissue. Restricted radiation was confirmed by phosphorylated histone 2AX expression in the non-radiated hemisphere 2 hours post treatment. Endotoxin low (≤0.001 EU/μg; ≤1 EU/mg) *and functional grade* rat anti-mouse immunoglobulin G $(IgG)_2b\kappa$ (isotype control), anti–PD-L1, and anti–programmed cell death protein 1 (PD1) (10 μg/g mouse body weight) were administered starting on the day of radiation (post tumor initiation day 15) and then daily until endpoint. Bioluminescence signals were obtained for each treatment group every 2–3 days following treatment. The last bioluminescence signal represents the last time point measured prior to reaching endpoint (see Kaplan–Meier curve for endpoints). Animals were sacrificed upon development of neurologic symptoms as defined by the Institutional Animal Care and Use Committee.

Bioluminescence and MRI

Bioluminescence imaging was obtained on the Xenogen IVIS 100 system. Mice with tumors expressing luciferase were anesthetized with isoflurane before intraperitoneal injection with 75 mg/kg body weight D-luciferin (Caliper Life Sciences #119222). Ten minutes after injection, images were acquired for 3–5 mins. Total flux (photons $seconds^{-1}$) was obtained from each mouse. An MRI scan (Bruker 1T scanner) was obtained immediately after or just prior to bioluminescence to delineate tumor and inflammation. Mice were imaged on this combination protocol the first day of treatment and 3, 5, 10, 14, and 21 days after treatment. Volumes of interest were manually contoured along the T2-hypertense rim of tumors for all animals on Viviquant software (Invicro).

Standard Immunohistochemistry

Mouse brains were fixed in formalin and embedded in paraffin, then sectioned at 5 μm and stained by routine hematoxylin and eosin, as well as immunohistochemistry (IHC). Automated IHC was performed on the Discovery XT (Ventana Medical Systems) instrument according to the manufacturer's standard protocol.

In Vitro Fluorescent Labeled Bacteria Phagocytosis

Following 8 hours of serum starvation, mouse macrophages were treated with specific antibodies for 24 hours. The effect of anti–PD-L1 antibodies on macrophage phagocytosis was assessed using the Vybrant Phagocytosis Assay Kit (Thermo Fisher #V-6694).

Selective Extracellular Signal-Regulated Kinase 1 and 2 Pathway Inhibition

The selective extracellular signal-regulated kinase (ERK)1/2 inhibitor PD98059 was purchased from Cell Signaling Technology (#9909). For the in vitro studies, macrophages were serum starved for 8 hours and pre-incubated in specified concentrations of PD98059 one hour prior to addition of anti–PD-L1 antibodies (20 μg/mL). For western blot (ERK phosphorylation), cell lysates were obtained at 30 minutes and 3 hours following treatment with anti–PD-L1 antibodies (mouse anti–PD-L1 from BioXCell; human: avelumab from Merck and atezolizumab from Genentech).

Differentiation of Monocytes into Macrophages In Vitro

At least 3 biological replicates were used in each mouse macrophage experiment, while donor human peripheral monocyte derived macrophages were evaluated per antibody tested. To obtain enough starting mouse monocytes for macrophage differentiation, one mouse bone marrow derived macrophage biological replicate was derived from pooling bone marrow from the hind legs of 4 separate mice. Mouse bone marrow derived monocytes were harvested from *NTva; Ink4a/arf$^{-/-}$; Pten$^{flox/flox}$* mice and differentiated into macrophages with 50 μg/mL of macrophage colony stimulating factor (M-CSF) in Roswell Park Memorial Institute medium with 10% fetal bovine serum for 6 days. Mouse macrophages were replated at 5×10^5 cells per well (6-well plate) and allowed to rest overnight prior to treatments. Flow cytometry for cluster of differentiation (CD)11b, F4/80, PD-L1, and PD1 was performed to verify mouse bone marrow derived macrophages generated in vitro.

Antibody Depletion of T Cells

On post-tumor initiation days 10, 15, 19, 22, and 30, tumor-bearing mice were treated with 0.4 mg of depleting antibodies via the intraperitoneal route: rat anti-mouse $IgG_2b\kappa$ (isotype control, BioXCell #BE0090), rat anti-CD4 (GK1.5 clone, BioXCell #BE0003-1), and rat anti-CD8 (2.43 clone, BioXCell #BE0061). Spleens ($n = 2$) were harvested from each treatment group on post-tumor initiation day 22 and evaluated by flow cytometry for T-cell depletion using the following antibodies: CD8-PE (Biolegend #100708) and CD4-APC (Biolegend #100515).

Nanostring Gene Expression Analysis

Conditions for Nanostring gene expression profiling were untreated and anti–PD-L1 (20 μg/mL). Conditions for real-time PCR verification were isotype control (negative control), lipopolysaccharide (positive control; Sigma #L3024), anti–PD-L1 (20 μg/mL), and soluble recombinant human PD1-fc (20 μg/mL). Following specified treatment for 200 minutes, media were aspirated, cells were rinsed in sterile phosphate buffered saline and lysed in RLT (Qiagen #1015750) + 1% BME (2-Mercaptoethanol) (Bio-Rad #161-0710) at 3500 cells/μL per Nanostring recommendations.

PCR samples were lysed in 350 μL. The mouse myeloid innate immunity panel (XT-PGX-MMV2-Myeloid, Nanostring #11500181) was used to assess the expression of immune-related genes following treatment per Nanostring protocol.

Statistical Analysis

Statistical analysis was performed using GraphPad Prism 7 software. Data were expressed as mean (SEM). Two-sided Man-Whitney *U*-tests and Holm-Bonferroni multiple comparison post hoc tests were performed to compare groups, as applicable. For survival studies, Kaplan–Meier analysis was performed using the log-rank (Mantel–Cox) test. A P-value < 0.05 was considered statistically significant.

Results

Effects of Anti–PD-L1 and Anti-PD1 Immunotherapy on Survival of Bilateral PDGF-Driven Glioblastoma-Bearing Mice Following Unilateral Radiation Therapy

To visualize and optimize the abscopal response for glioblastoma in vivo, we generated 2 genetically distinct PDGF-driven glioblastomas within the brain. In one hemisphere, we induced a glioblastoma driven by PDGF-shPten, while in the other hemisphere we generated a PDGF-driven glioblastoma with luciferase expression (Ntva Ink4a/Arf$^{-/-}$ Pten$^{flox/flox}$ mice with *Lox-Stop-Lox* Luciferase; Fig. 1A) via deletion of the *Lox-STOP-Lox* sequence through injection of RCAS-Cre only in one side (Fig. 1A, top). To evaluate the influence of specific tumor neoepitope expression during an abscopal response, we induced unilateral expression of EGFRvIII, which contains the unique fusion junction peptide LEEKKGNYVVTDH (Ntva Ink4a/Arf$^{-/-}$ Pten$^{flox/flox}$ mice with *Lox-Stop-Lox* EGFRvIII; Fig. 1A) via deletion of the *Lox-STOP-Lox* sequence through injection of RCAS-Cre only in one side (Fig. 1A, bottom). In the PDGF-luciferase (PDGF + Luc) mice, restriction of luciferase expression to one hemisphere (the non-radiated side) allowed the unilateral bioluminescence readout of tumor cell viability following radiation of the other hemisphere. Radiation-induced damage was restricted to the radiated hemisphere as determined by phospho-histone 2A.X immunostaining 2 hours post radiation treatment (Supplementary Fig. 1A). Post radiation tumor growth was assessed in vivo by two methods: (i) MRI to visualize bilateral tumor growth (Fig. 1B, left) and (ii) bioluminescence as a readout of tumor cell viability on the non-radiated hemisphere (Fig. 1B, right. Correlation between MRI and bioluminescence is in Fig. 1C; $R^2 = 0.9649$).

We then assessed how checkpoint inhibition could functionally enhance targeted immune response to unirradiated tumor in vivo by determining the relative effects of systemic anti–PD-L1 and anti-PD1 immunotherapy (either daily 10 μg/g anti–PD-L1 or anti-PD1) on survival when combined with unilateral radiation. Administration of anti–PD-L1 immunotherapy in conjunction with unilateral radiation resulted in a modest improvement in survival in PDGF + Luc glioblastoma (n = 7–8/group, median survival = 40.5 days vs radiation alone 37.5 days, log-rank $P = 0.03$; Fig. 1D). In PDGF + EGFRvIII glioblastoma, there was increased improvement in survival following anti–PD-L1 immunotherapy and unilateral radiation (n = 8/group, median survival = 36 days vs radiation alone 28 days, log-rank $P = 0.001$: Fig. 1E). In a one-sided brain tumor model, 10 Gy unilateral radiation to nontumor brain had no effect on survival (Supplementary Fig. 1B, C). This indicated that combination therapy (radiation and systemic anti–PD-L1) was superior to monotherapy (systemic anti–PD-L1 alone) in the RCAS/TVA glioblastoma mouse model. Of note, this response occurs in the absence of significant PD-L1 expression within the PDGF + Luc or PDGF + EGFRvIII microenvironment (Supplementary Fig. 2A, B for multiplexed IHC).

Comparison of Bioluminescence Activity with Brain MRI for In Vivo Measurement of Tumor Cell Viability Following Combined Glioblastoma Therapy

To determine if the enhanced survival benefit from combined radiation and anti–PD-L1 immunotherapy is associated with reduction of tumor cell viability on the contralateral non-radiated side, we compared changes in routine MRI signal, representing tumor volume and inflammation, with luciferase activity, representing tumor viability in the PDGF + Luc model. In IgG control treated animals, an increase in unirradiated tumor growth corresponded with increased MRI signal (n = 8/8; Fig. 2B). As a positive control, whole brain radiation with 10 Gy caused a decrease in both MRI signal and luciferase activity (n = 4/4; Fig. 2B). Monotherapy with daily systemic anti–PD-L1 antibodies (10 μg/g) had no impact on tumor progression based on MR imaging or luciferase activity (n = 0/4; Fig. 2B). Unilateral radiation alone resulted in continued tumor growth as measured by MRI in all cases, but a subset of these tumors concurrently showed a small but not significant decrease in viable tumor cell numbers as measured by reduced luciferase activity, indicating a potential abscopal effect for unilateral radiation alone occurring in only a few treated animals (n = 2/4; Fig. 2B). Conversely, concurrent daily systemic anti–PD-L1 immunotherapy enhanced this abscopal effect of 10Gy radiation on the un-irradiated, luciferase-containing tumor. This combined therapy resulted in a decrease of tumor cell viability in 8/8 mice (100%) and an increase in MRI signal in 5/8 mice (62.5%; Fig. 2B. Tumor cell viability or luciferase activity for all groups is shown in Fig. 2C). The discordance between loss of viable tumor cell and increased tumor size may represent treatment-induced inflammation (pseudoprogression) and/or edema falsely mimicking tumor progression on MRI. These results suggested that, following radiation and anti–PD-L1 immunotherapy, regression of unirradiated lesions may contribute to improved survival in the bilateral brain tumor model.

Effect of Anti–PD-L1 Immunotherapy on Radiation Therapy–Mediated Recruitment of Macrophages and T Cells into Brain Tumors

To investigate the relevance of tumor neoepitope expression during the abscopal response, we histologically quantified macrophage (ionized calcium binding adaptor

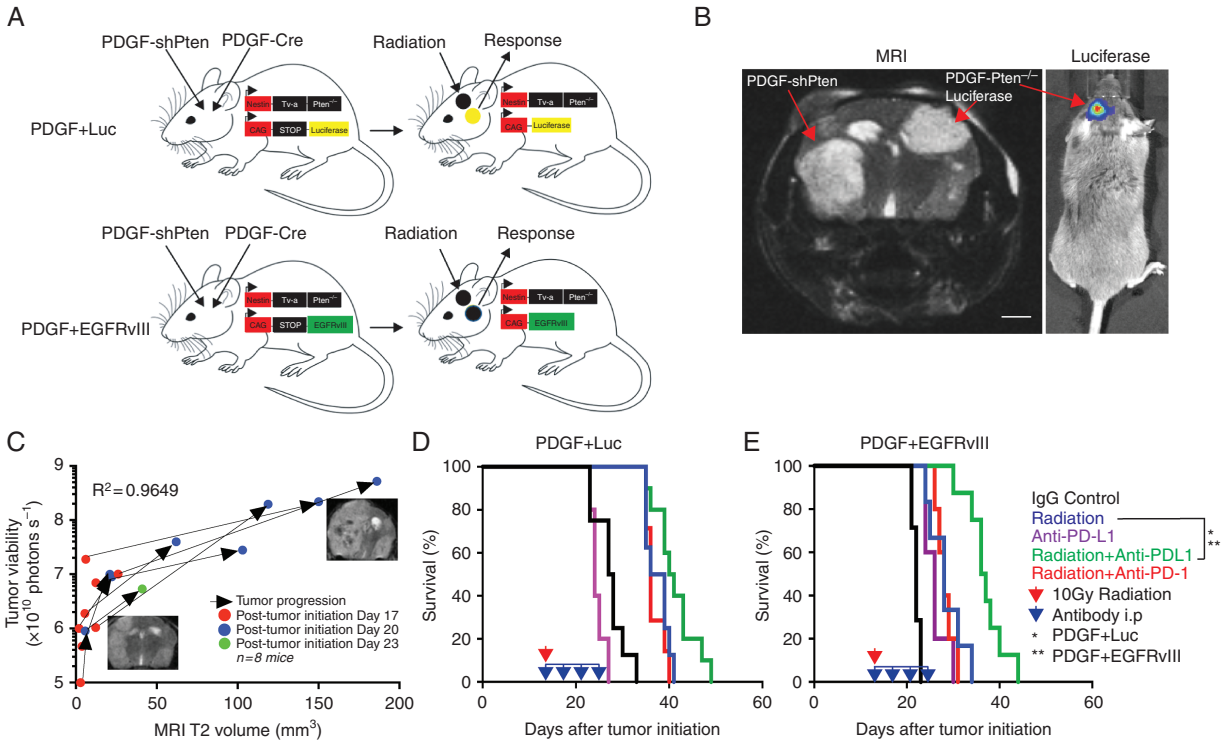

Fig. 1 Combined unilateral radiation and systemic anti–PD-L1 immunotherapy increase survival in a bilateral glioblastoma model. (A) Strategy for inducing mouse bilateral glioblastoma within the brain using the RCAS/TVA mouse model for immune microenvironment profiling and Cre-recombination strategy used to generate unilateral luciferase expressing PDGF + Luc (top) and PDGF + EGFRvIII (bottom) tumors (Tg(NES-TVA);*Cdkn2a (Ink4a-Arf)*$^{-/-}$;*Pten*$^{fl/fl}$; LSL Luciferase and EGFRvIII mice). (B) Representative MRI (left panel) of a bilateral glioblastoma mouse model. Right panel is bioluminescence signal from mouse in left panel, showing unilateral luciferase activity from the left-sided PDGF-*Pten*$^{-/-}$ tumor only. Red arrows delineate tumors on each side of brain. Scale bar = 1 mm. (C) Correlation between tumor viability (luciferase activity) and MRI T2-weighted signal in IgG-treated animals bearing bilateral glioblastoma (n = 8 mice, R^2 = 0.9649). Two to 3 representative MRI scans highlighting interval growth in one untreated animal with arrows showing direction of growth between scans. Red circles are measurements from time point 1 (post-tumor initiation day 17), blue circles are measurements from time point 2 (post-tumor initiation day 20), and green circles are measurements from time point 3 (post-tumor initiation day 23). *Y*-axis in logarithmic scale (photons second^{-1}). *X*-axis in linear scale (mm^3). (D–E) Kaplan–Meier survival curves showing that anti–PD-L1 immunotherapy enhances unilateral radiation-induced survival in bilateral PDGF + Luc (D) and PDGF + EGFRvIII (E) glioblastoma (n = 6–8 mice per treatment group). Red arrow indicates unilateral 10 Gy irradiation. Blue arrow indicates daily anti–PD-L1 or anti-PD1 treatments. Treatments began on post-tumor initiation day 15. Log-rank Mantel–Cox test for radiation alone versus radiation with anti–PD-L1. *P < 0.05 for PDGF + Luc, **P < 0.01 for PDGF + EGFRvIII.

molecule 1 [Iba1+]) and T-cell (CD3+) infiltration into tumors on both irradiated and unirradiated sides of both glioma models (PDGF + Luc and PDGF + EGFRvIII) after treatment with radiation and anti–PD-L1 immunotherapy on posttreatment day 10. Relative to IgG isotype control (n = 5), 10 Gy radiation and daily anti–PD-L1 immunotherapy (n = 5) induced a significant macrophage (P < 0.0001) and T-cell (P < 0.0001) infiltration into both unirradiated and radiated sides of PDGF + EGFRvIII gliomas (Fig. 3A–D, F). In PDGF + Luc gliomas (n = 5), relative to IgG isotype control (n = 5), there was an absence of T-cell infiltration (P > 0.05). However, a macrophage-predominant response was noted in both unirradiated (P < 0.0001) and irradiated tumors (P < 0.0001) (Fig. 3A–E). These results indicated that following radiation and anti–PD-L1 immunotherapy, the slightly higher survival advantage noted in the neoepitope expressing PDGF + EGFRvIII glioma-bearing mice (relative to the PDGF + Luc glioma mice) may be due to an inherent ability to recruit T cells into unirradiated and irradiated tumors.

In PDGF + Luc gliomas (lacking tumor neoepitope), systemic depletion of circulating CD4+ and CD8+ T cells did not affect the survival benefit associated with radiation combined with anti–PD-L1 immunotherapy (Fig. 4 A–C). Therefore, to investigate the impact of macrophage recruitment on glioma growth independent of T-cell activation, we sought the source of tumor-infiltrating macrophages following radiation and anti–PD-L1 immunotherapy. We generated bilateral PDGF-*Pten*$^{-/-}$ glioblastoma (lacking tumor neoepitope) in the *NTva; Cdkn2a*^{wt}*; Pten*$^{flox/flox}$*; CX3CR1*$^{+/GFP}$*; CCR2*$^{+/RFP}$ mouse model. Here, *CX3CR1*$^{+/GFP}$ and *CCR2*$^{+/RFP}$ delineate microglia (green fluorescent protein [GFP+]) and peripheral monocytes (red fluorescent protein [RFP+]), respectively, and double positive CX3CR1$^{+/GFP}$/CCR2$^{+/RFP}$ delineates peripherally derived tumor-associated macrophages (GFP+/RFP+).[13] Relative to radiation alone (n = 6), the addition of daily anti–PD-L1

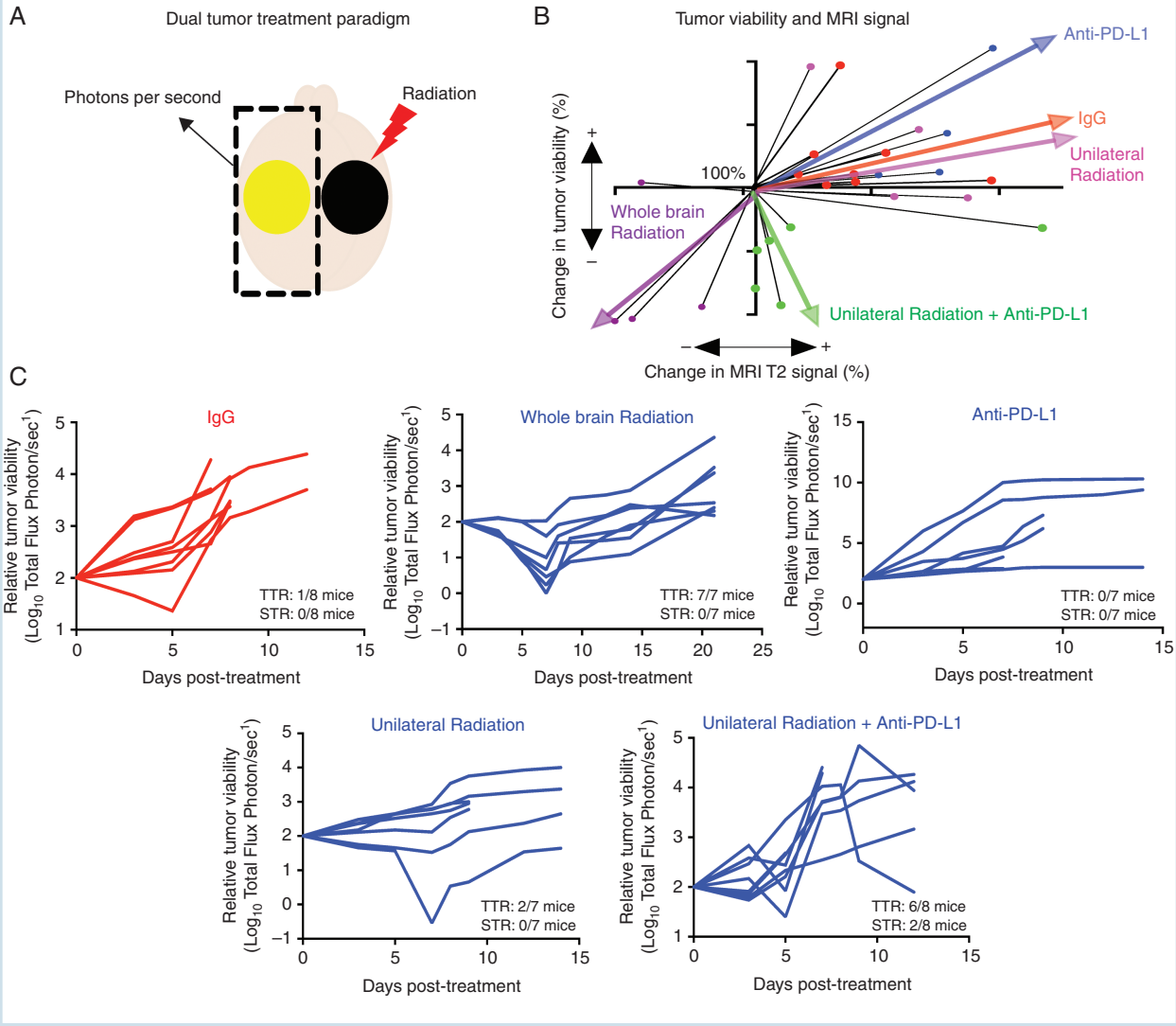

Fig. 2 Abscopal effect of combined localized radiation and systemic anti–PD-L1 immunotherapy. (A) Depiction of experimental strategy of bilateral mouse glioblastoma to measure abscopal effect in Tg(*NTva*);*Ink4a-Arf*$^{-/-}$;*Pten*$^{-/-}$; LoxP-Stop-LoxP luciferase mice with left-sided PDGF-*Pten*$^{-/-}$ luciferase tumor and right-sided PDGF-shPten tumor. The right hemisphere contains a non-luciferase tumor and is irradiated. The left side contains neoplastic cells harboring luciferase expression and is not irradiated. Tumor viability (photons second^{-1}) and MRI tumor volume (mm^3) are obtained from the left-sided, non-irradiated tumor only. (B) Association between tumor viability (photons second^{-1}) and MRI tumor volume (mm^3) for all treatment groups. The growth pattern of each individual animal is shown as black lines and the linear regression summation of all the animals in the treatment group are depicted as colored wide arrows. Mice receiving combination imaging included IgG control ($n = 8$, red), whole brain radiation ($n = 4$, purple), non-luciferase tumor radiation alone ($n = 4$, magenta), anti–PD-L1 alone ($n = 4$, blue), and non-luciferase tumor radiation with anti–PD-L1 ($n = 8$, green). Tumor viability (luciferase activity in photons second^{-1}) and MRI T2 signal volume (mm^3) are shown relative to pretreatment starting point that was normalized to 100% for all mice. (C) Response of unirradiated tumor to treatment is categorized as transient tumor regression (TTR) or sustained tumor regression (STR). TTR represents any decrease in unirradiated tumor viability (luciferase activity) that is followed by unirradiated tumor regrowth. STR represents any decrease in unirradiated tumor viability that is not followed by unirradiated tumor regrowth prior to reaching endpoint. Relative to IgG treated animals (red), whole brain radiation (10 Gy) or radiation positive control induces TTR in 7 of 7 mice, with STR in 0 of 7 mice. Anti–PD-L1 antibody alone does not induce TTR or STR in any mice (0 of 7 mice). Unilateral radiation of non-luciferase expressing tumor induces TTR in 2 of 7 mice, with STR in 0 of 7 mice. Unilateral radiation of non-luciferase tumor and anti–PD-L1 antibodies induces TTR in 6 of 8 mice, with STR in 2 of 8 mice. All posttreatment viability is shown relative to the original tumor viability, with growth showing increase and treatment response showing decrease on a $\log_{10}$ scale. IgG isotype control is the same for all treatment groups and is shown in red, relative to experimental group shown in blue.

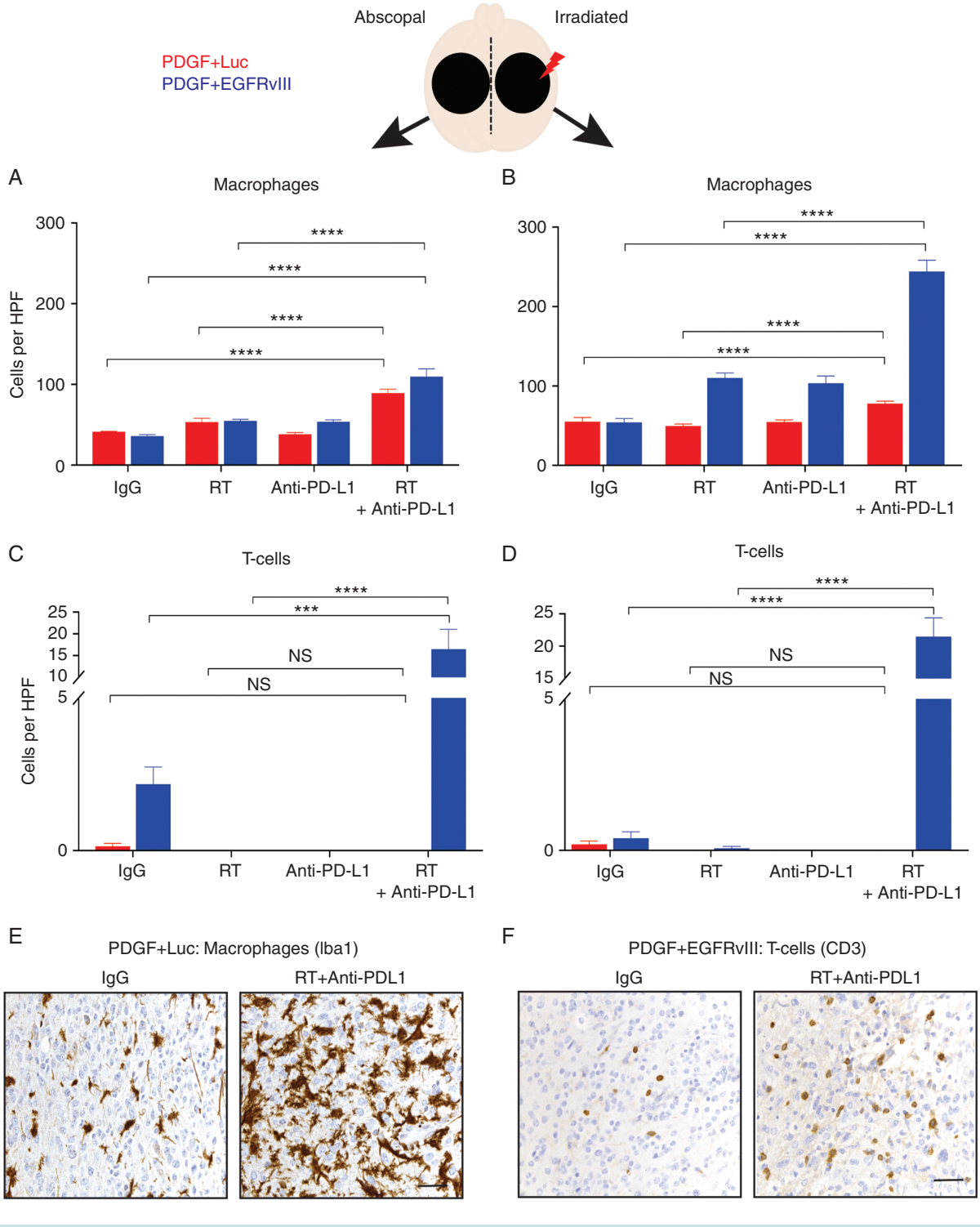

Fig. 3 Localized radiation and systemic anti–PD-L1 immunotherapy promote intratumoral macrophage and T-cell infiltration. (A, B) Quantification of Iba1+ macrophage influx into unirradiated or abscopal side (A) and radiated side (B) based on IHC on PDGF + Luc (red) and PDGF + EGFRvIII (blue) mouse gliomas on posttreatment day 10, $n = 5$ mice per group. (C, D) Quantification of CD3+ T-cell macrophage influx into unirradiated or abscopal side (C) and radiated side (D) based on IHC on PDGF + Luc (red) and PDGF + EGFRvIII (blue) mouse gliomas following treatment, $n = 5$ mice per group. (E, F) Representative IHC for macrophages (Iba1) in PDGF + Luc gliomas (E) and T cells (CD3) in PDGF + EGFRvIII gliomas (F) following treatment (abscopal side). Three to 5 high-powered fields were counted per tumor sample from 5 different tumors on posttreatment day 10. Scale bar = 50 μm. *P*-values derived from the non-parametric Mann–Whitney *U*-test, two-sided. Holm–Bonferroni multiple comparison post hoc test for A–D. Error bars = SEM. $^{*}P < 0.05$, $^{**}P < 0.01$, $^{***}P < 0.001$, $^{****}P < 0.0001$, NS = not significant.

immunotherapy to unilateral 10 Gy radiation ($n = 6$) significantly increased the numbers of double positive CX3CR1$^{+/GFP}$/CCR2$^{+/RFP}$ circulating monocyte-derived macrophages in both unirradiated (median increase 40%, $P < 0.01$) and irradiated bilateral tumors on posttreatment day 5 (median increase 30%, $P < 0.01$) (Fig. 4D, E; flow cytometry gating strategy is in Supplementary Fig. 3A). It also demonstrated a loss of microglia (shown as a percentage of viable cells) within the irradiated tumor, consistent with a known consequence of direct radiation on the tumor microenvironment.[14] Further investigation of this macrophage response showed that, similar to human glioblastoma,[15] RCAS/TVA glioblastoma-bearing mice demonstrated elevated levels of immunosuppressive PD-L1+/Ly6C+ monocytes in peripheral blood relative to healthy nontumor mice ($n = 5$ per PDGF + Luc or PDGF + EGFRvIII healthy and tumor mice) ($P < 0.01$) (Supplementary Fig. 3B; flow cytometry gating strategy is in Supplementary Fig. 3C). Following a combination of radiation and anti–PD-L1 immunotherapy, flow cytometry of tumors from PDGF-*Pten*$^{-/-}$ glioblastoma in the CX3CR1$^{+/GFP}$/CCR2$^{+/RFP}$ model demonstrated that, relative to radiation alone ($n = 6$), combining radiation with daily anti–PD-L1 immunotherapy ($n = 6$) increased the fraction of Ly6C+ immune cells (shown as percentage of all viable cells) within both irradiated and unirradiated tumors on posttreatment day 5 ($P < 0.01$) (Supplementary Fig. 3D; flow cytometry gating strategy is in Supplementary Fig. 3F). Further, increased levels of the PD-L1+/Ly6C+ subpopulation infiltrated the non-irradiated tumor ($P < 0.05$) (Supplementary Fig. 3E; flow cytometry gating strategy is in Supplementary Fig. 3F). These data suggested that the combination of radiation and anti–PD-L1 immunotherapy enhanced recruitment of bone marrow–derived immunosuppressive PD-L1+ monocytes into adjacent unirradiated glioblastoma as tumor-associated macrophages.

Effect of Anti–PD-L1 Antibodies on Monocyte-Derived Macrophage Activation In Vitro

Previous research has shown that anti-PD1 antibody direct activation of PD1+ macrophages, independently of T-cell activation, results in a pro-inflammatory, antitumor phenotype in tumor-associated macrophages.[16] Therefore, we investigated whether anti–PD-L1 antibodies could also directly induce an antitumor phenotype in bone marrow–derived PD-L1+ macrophages ex vivo. Incubation of bone marrow–derived M-CSF differentiated PD-L1+/CD11b+/F4/80+ macrophages (Supplementary Fig. 4A; flow cytometry gating strategy is in Supplementary Fig. 4B) with anti–PD-L1 antibodies induced a shift in gene expression in mouse macrophages in vitro (Supplementary Table 1). Upregulation of 95 myeloid-related genes, and downregulation of 44 genes, was induced with anti–PD-L1 treatment (Supplementary Table 2). Most of these genes were related to an increase in cell cycle and cytokine production (Fig. 5A, B). There was evidence of signaling associated with both activation and inhibition of macrophage function (Supplementary Table 2) indicating that subsequent macrophage phenotype is dependent on the balance between pro-inflammatory and pro-tumor gene expression or signaling pathways. Targeted myeloid-related gene expression was validated by real-time quantitative PCR using an isotype negative control (IgG_2b), lipopolysaccharide as positive control, Fc conjugated soluble PD1 (IgG_1 isotype), and anti–PD-L1 antibody (IgG_2b isotype). Relative to isotype control, anti–PD-L1 induced significant increases in pro-inflammatory gene expression in macrophages (Olr1, Cxcl3, and Ccl3; $P < 0.01$) (Supplementary Fig. 4C and Supplementary Tables 3 and 4). Soluble PD1 was equally effective at inducing pro-inflammatory gene expression changes relative to anti–PD-L1 antibody, illustrating the on-target effects of anti–PD-L1 ($P < 0.01$) (Supplementary Fig. 4C).

Effect of Anti–PD-L1 Antibodies on Macrophage Phagocytic Activity via ERK Pathway Activation

Gene ontology on the Nanostring gene expression data was indicative of both activation and inhibition of the ERK pathway following incubation of PD-L1+/PD1– mouse macrophages with an anti–PD-L1 antibody, with more significance in ERK activation signaling pathways (Fig. 5A). To further explore this, we expanded the treatment regimen of mouse macrophages in vitro to include 2 clinical grade human anti–PD-L1 antibodies: avelumab and atezolizumab. All mouse and human anti–PD-L1 antibodies induced ERK phosphorylation in their respective macrophages in vitro (Fig. 5C–F). This effect was not observed when PD-L1 treated macrophages were exposed to the selective ERK inhibitor PD98059 (Fig. 5C–F). Functionally, anti–PD-L1 antibodies also significantly enhanced macrophage in vitro phagocytic activity ($P < 0.0001$) (Fig. 6A). This phagocytic effect driven by anti–PD-L1 was reversed by pretreatment of the macrophages with the selective ERK inhibitor PD98059 ($P < 0.0001$) (Fig. 6A). In vivo, following radiation and anti–PD-L1, there was also increased phagocytosis of tumor cells based on IHC colocalization of oligodendrocyte transcription factor 2 (Olig2+) tumor cells within Iba1+ macrophages in both irradiated and unirradiated low baseline intratumoral PDGF + Luc glioblastoma ($P < 0.01$) (Fig. 6B, C). Anti–PD-L1 treatment alone did not increase phagocytosis of tumor cells in vitro (data not shown). This indicated that following a radiation-induced recruitment of the immunosuppressive PD-L1+ monocytes to brain tumors, anti–PD-L1 antibodies directly induced a pro-inflammatory and antitumor phenotype in PD-L1+ tumor-infiltrating macrophages, resulting in enhanced phagocytosis of tumor cells in the periphery of the prior radiation site.

Discussion

The specific mechanism mediating the abscopal phenomenon remains an enigma. Based on a meta-analysis, the relative contribution of antigen-presenting cells (APCs) such as macrophages, dendritic cells, or T cells to the abscopal response varies depending on radiation schedule, dosage, animal model, or immune checkpoint inhibitor used.[17] Prior to T-cell activation during the abscopal response, radiation-induced tumor death results in release of neoantigens or neoepitopes which are engulfed by APCs.[18] APCs then circulate to lymph nodes where neoantigen

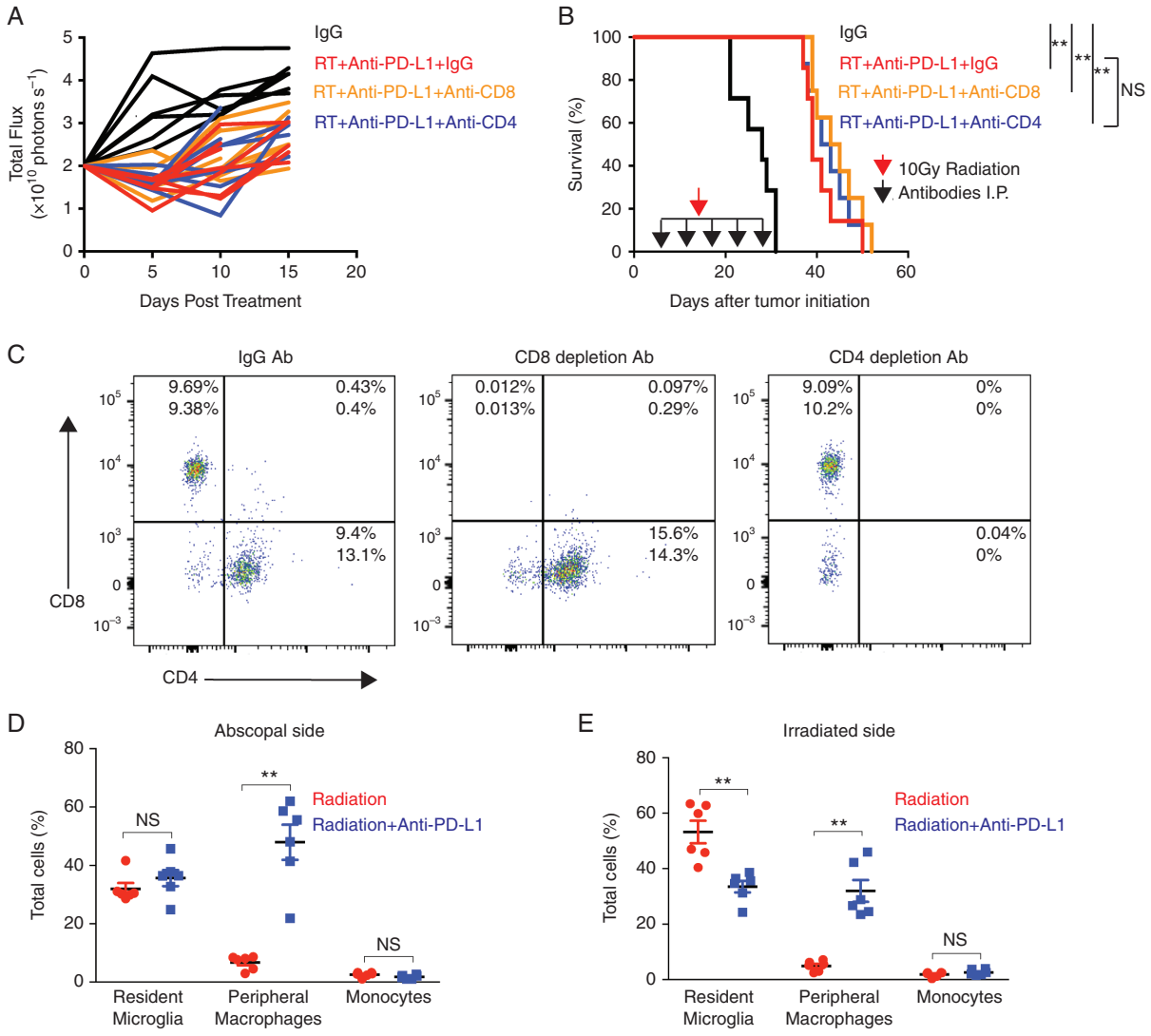

Fig. 4 T-cell depletion does not affect abscopal effect in PDGF + Luc glioblastoma. (A, B) Bioluminescence (A) and survival data (B) from Tg(*NTva*);*Ink4a-Arf*$^{-/-}$;*Pten*$^{-/-}$; LoxP-Stop-LoxP luciferase mice with left-sided PDGF-*Pten*$^{-/-}$ luciferase tumor and right-sided PDGF-shPten tumor treated with anti-mouse IgG_2b isotype control ($n = 7$), anti-CD8 ($n = 8$), and anti-CD4 ($n = 8$) depleting antibodies at 10, 15, 19, 22, and 30 days post-tumor initiation (black arrows in B). Unilateral 10 Gy radiation was then administered (red arrow in B) followed by daily anti–PD-L1 therapy. Based on luciferase activity measured within 10 days post treatment initiation, abscopal response seen in 7/7 IgG treated mice, 8/8 CD8+ T-cell depleted mice, and 8/8 CD4+ T-cell depleted mice. Survival curves following T-cell depletion in radiation and anti–PD-L1 treated mice showing no impact of T-cell depletion on survival (B). Log-rank Mantel–Cox test for radiation alone versus radiation with anti–PD-L1. $^{**}P < 0.01$, NS = not significant. (C) To verify T-cell depletion, flow cytometry was performed on spleens harvested from mice receiving combination therapy ($n = 2$ per group) on post-tumor initiation day 22 after 2 doses of depleting antibodies demonstrating >90% depletion. (D, E) On posttreatment day 5, relative to radiation alone ($n = 6$, red), combination immunotherapy with anti–PD-L1 ($n = 6$, blue) is associated with increased infiltration of bone marrow–derived macrophages (CX3CR1$^{+/GFP}$/CCR2$^{+/RFP}$) into the non-irradiated/abscopal side as shown in D, and the irradiated side as shown in E, of bilateral RCAS-PDGF–driven glioblastoma in *Ntva; Cdkn2a*^{wt}*; Pten*$^{flox/flox}$*; CX3CR1*$^{+/GFP}$*; CCR2*$^{+/RFP}$ mice. Red circles are unilateral radiation treated mice, blue squares are unilateral radiation and anti–PD-L1 treated mice. *P*-values derived from the non-parametric Mann–Whitney *U*-test, two-sided. Error bars = SEM. $^{**}P < 0.01$, NS = not significant.

presentation results in activation and education of naïve T cells. Activated and tumor-specific T cells enter the circulation and selectively target tumor cells, resulting in regression of unirradiated tumors.

Even though the abscopal response is well known in other cancer types, the complete mechanism mediating immune recognition of untreated tumors remains an enigma.[17] Our results indicate that glioblastomas with neoepitopes, such as EGFRvIII tumors, may be more susceptible to an immunologically mediated abscopal response, although the functional significance of T-cell infiltration or neoepitope type for survival is currently being

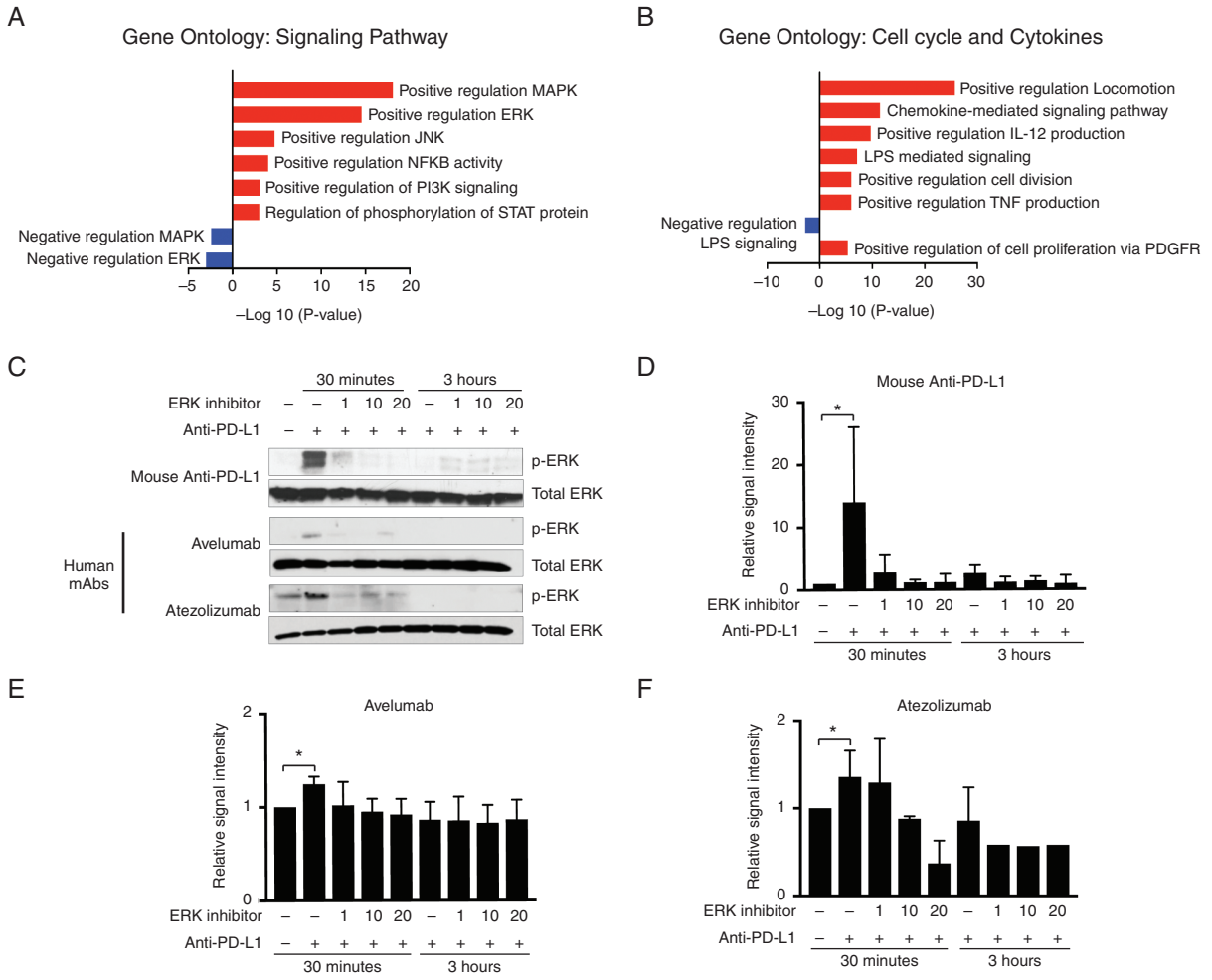

Fig. 5 Anti–PD-L1 antibodies directly activate bone marrow–derived macrophages. (A, B) Gene ontology analysis of differentially expressed genes following incubation of anti–PD-L1 antibodies with macrophages in vitro. Cell signaling pathways are shown in A and cell cycle/cytokine activation is shown in B. We noted both activating and inhibitory signaling following anti–PD-L1 treatment of macrophages in vitro (red, upregulation; blue, downregulation). Gene expression is based on average fold change from mouse bone marrow–derived macrophages from 3 different mice pools. (C–F) Anti–PD-L1 antibodies induce ERK phosphorylation (p44/42) in mouse bone marrow–derived macrophages, quantified in D, and human peripheral blood monocyte–derived macrophages, quantified in E and F. Lysates were collected at 30 minutes and 3 hours posttreatment with anti–PD-L1 antibodies. Two clinical grade human monoclonal antibodies (mAb) were evaluated including avelumab (Bavencio, Merck) and atezolizumab (Tecentriq, Genentech). Selective ERK inhibition with PD98059 (Cell Signaling) is shown in a dose-dependent manner. Matched isotype antibody was used as a negative control. Total ERK is the loading control. Results were independently replicated in different mouse bone marrow–derived macrophages from 3 different mice pools and 2 different healthy human peripheral blood mononuclear cell donors.

investigated. A majority of glioblastomas, however, lack neoepitope expression.[19] Therefore, uncovering strategies that enhance the immunologic response to glioblastoma in the absence of neoepitope-associated T-cell recruitment may improve survival. Direct activation of macrophages has been associated with the abscopal response in the absence of T-cell infiltration.[20–22] Given the critical role of macrophages demonstrated in the response to immunotherapy in our model, a better understanding of mechanisms that could enhance the macrophage-dependent abscopal effect is warranted. One possibility is the release of inflammatory cytokines or death associated molecular patterns from dying tumor cells.[18,21,22] Following radiation-induced recruitment to the brain, infiltrating macrophages are polarized by anti–PD-L1 antibodies into antitumor states resulting in eradication of previously viable tumor cells just outside of the irradiated area (the bystander effect). A second possibility is that macrophages are "educated" by tumor antigens released following irradiation, resulting in a tumor-specific response. The mechanism behind this macrophage "education," however, remains unknown and warrants further investigation.

Although blockades of PD1 and PD-L1, respectively, are often thought of as equivalent, the effect of anti-PD1 in our mouse model is not similar to that of anti–PD-L1. One reason for this phenotypic

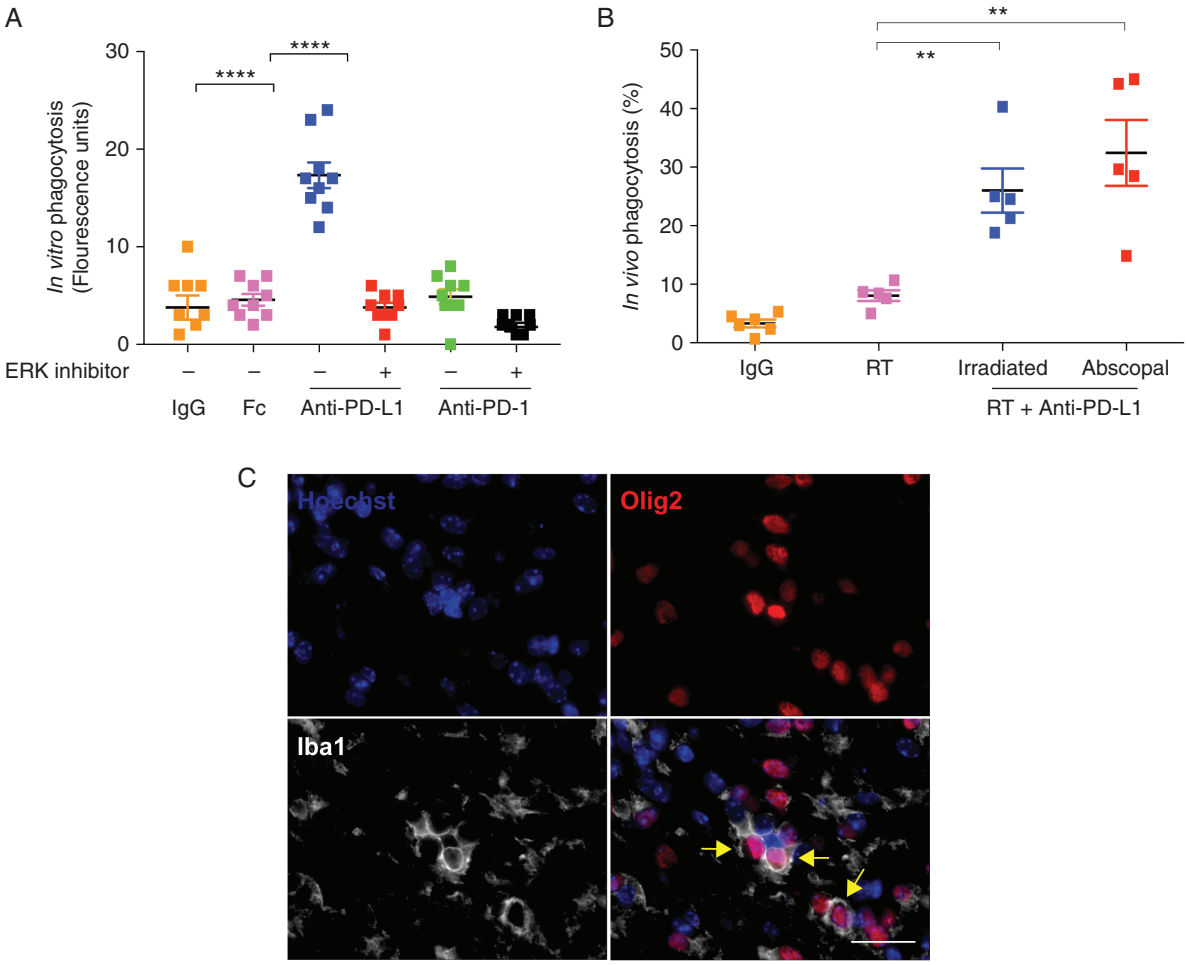

Fig. 6 Anti–PD-L1 enhances macrophage phagocytosis in PDGF + Luc gliomas. (A) Anti–PD-L1 antibodies promote phagocytosis of fluorescein isothiocyanate–labeled *Escherichia coli* particles in vitro via ERK signaling in PD-L1+/PD1– murine macrophages. Phagocytosis of the particles was measured by a Vybrant Phagocytosis Assay Kit. This anti–PD-L1 effect on macrophages is inhibited by PD98059, an ERK inhibitor (20 μM). Three biological replicates each with 3 technical replicates are shown. Orange are IgG controls, pink is FcγR (CD16/32) receptor block, blue is anti–PD-L1 without ERK inhibitor, red is anti–PD-L1 with ERK inhibitor, green is anti-PD1 without ERK inhibitor, black is anti–PD-L1 with ERK inhibitor. (B) Percent phagocytosis represents the proportion of Iba1+ cells (macrophages) that have circumferentially encircled an Olig2+ neoplastic cell. Counts from at least 5 high-powered fields (40x objective) per animal from posttreatment day 10. Each point represents a single animal with bilateral tumors from PDGF + Luc glioblastoma ($n = 5$–6 mice per treatment group). Orange is IgG control, pink is unilateral radiation only, blue is the irradiated side of anti–PD-L1 with unilateral radiation, red is the abscopal side of anti–PD-L1 with unilateral radiation. (C) Representative immunofluorescence microscopy for Hoechst (all nuclei), Olig2 (neoplastic cells), and Iba1 (macrophages) in PDGF + Luc (radiated side) mouse glioblastoma on posttreatment day 10. Yellow arrows indicate phagocytosed Olig2+ neoplastic cells (magnification 40x; scale bar = 30 μm). *P*-values derived from the non-parametric Mann–Whitney *U*-test, two-sided. Error bars = SEM. $^{**}P < 0.01$, $^{****}P < 0.0001$, NS = not significant.

distinction is that anti–PD-L1 seems to directly activate PD-L1+ macrophages to increase production of cytokines and enhance phagocytosis in an ERK signaling–dependent manner. Since glioblastomas are enriched with macrophages (20–30% of tumor mass),[23–26] these immune cells may serve as better agents for achieving an immune-induced therapeutic effect. In some late stage cancer types, anti-PD1 also activates phagocytosis in some tumor-associated macrophages,[16] an effect dependent on expression of PD1 by these macrophages. In glioblastoma there is little PD1 expression within the tumor and on circulating monocytes of tumor-bearing mice. By contrast, PD-L1 is expressed at higher levels on circulating monocytes of tumor-bearing mice and human glioblastoma patients.[15] A recent report showed that anti–PD-L1 antibodies directly activate bone marrow–derived macrophages in vitro,[27] indicating that similar to anti-PD1, anti–PD-L1 activated macrophages could also mediate an antitumor response independently of T-cell activation. Given that macrophages are the largest immune cell population in glioblastoma and PD-L1+ circulating monocyte-derived macrophages are the cells that respond primarily to radiation therapy,[28] it is not surprising that after radiation therapy, mouse glioblastoma responds better to

anti–PD-L1 therapy, which specifically targets infiltrating PD-L1+ macrophages, than to anti-PD1 immunotherapy.

In our model, we also found that mice that received anti–PD-L1 monotherapy had poorer survival relative to IgG control treated mice. Although it remains unclear why this occurred, it indicates that without radiation therapy, anti–PD-L1 therapy may have a unique profile of targets and consequently a different outcome in tumor-bearing mice not receiving radiation therapy. Also because patients with PD-L1–negative tumors also respond to anti–PD-L1 therapy,[29] our results indicate that levels of PD-L1+ monocytes in circulation, not tumor PD-L1 expression, may be better prognostic indicators of response to anti–PD-L1 therapy following radiation for glioblastoma patients. To the degree that the mouse model reflects human biology, our results also suggest that patients with glioblastoma who fail anti-PD1 or anti–PD-L1 monotherapy could still respond to anti–PD-L1 combined with high-dose radiation of viable tumor cells.

Our study has several limitations. Since the gene expression profiling is based on macrophages cultured in vitro, it may not represent the macrophage phenotype in vivo; therefore, we plan to perform gene expression analysis from tumor cells and macrophages posttreatment in vivo. Also, given the limited specificity of C-C chemokine receptor 2 and CX3C chemokine receptor 1 as immune cell markers, we plan to perform lineage studies using fluorescence tagged bone marrow precursors to selectively track monocytes and macrophages following radiation and anti–PD-L1 therapy. The scope of genetic alterations assessed is also a limitation—therefore, we plan to assess the impact of other clinically significant mutations such as isocitrate dehydrogenase 1 mutation.

In summary, experimentally tractable models with representative histology in immune-competent mouse backgrounds are needed to optimize the abscopal effect for brain tumors. Such experimental systems also need to be robust at detecting, monitoring, and studying the abscopal effect in live animals following administration of diverse immunotherapeutic agents irrespective of route of administration. Using the RCAS/TVA system, we find that anti–PD-L1 immunotherapy enhances a radiotherapy-induced abscopal response. In tumors such as glioblastoma, where recurrence is driven by infiltrated tumor cells in the periphery of the radiation treatment regions, combinatorial strategies that induce an abscopal or bystander effect in patients will be critical for establishing local disease control and improving OS.

Supplementary Material

Supplementary data are available at *Neuro-Oncology* online.

Keywords

abscopal effect | glioblastoma | macrophages | radiation | T cells

Funding

This study was supported by the National Institute of Neurological Disorders and Stroke, National Institutes of Health (R25NS079200 to C.I.E.), and the National Cancer Institute, National Institutes of Health (U54CA193461–03 and R01CA195718–02 to E.C.H.). Swiss National Science Foundation, No. P2SKP3_158656 (to H.-G.W).

Acknowledgments

We would like to thank Jenny Zhang, Deby Kumasaka, and James Yan of the Holland laboratory for their assistance. We would also like to thank Jamie Nguyen of the Comparative Medicine facility at the Fred Hutchinson Cancer Research Center for assistance with imaging including bioluminescence and MRI scans. We would also like to thank Kimberly Smythe of Experimental Histopathology, Fred Hutchinson Cancer Research Center.

Conflict of interest statement. None.

Authorship statement. Conceptualization: C.I.E., E.C.H. Methodology: C.I.E., C.A.C., E.C.H. Investigation: C.I.E., S.A.K., M.J., H.Z., P.K., T.R.W., K.W.M. Data analysis: C.I.E., S.A., F.S., H.-G.W., P.J.C., J.B. Writing, original draft: C.I.E., E.C.H. Review and editing: C.I.E., P.J.C., A.P., S.J.D., C.A.C., E.C.H. Funding acquisition: I.F.P., C.A.C., E.C.H. Supervision: I.F.P., C.A.C., A.M.G., R.H.P., E.C.H.

References

1. Snuderl M, Fazlollahi L, Le LP, et al. Mosaic amplification of multiple receptor tyrosine kinase genes in glioblastoma. *Cancer Cell*. 2011;20(6):810–817.
2. Minniti G, Amelio D, Amichetti M, et al. Patterns of failure and comparison of different target volume delineations in patients with glioblastoma treated with conformal radiotherapy plus concomitant and adjuvant temozolomide. *Radiother Oncol*. 2010;97(3):377–381.
3. Mole RH. Whole body irradiation: radiobiology or medicine? *Br J Radiol*. 1953;26(305):234–241.
4. Crittenden M, Kohrt H, Levy R, et al. Current clinical trials testing combinations of immunotherapy and radiation. *Semin Radiat Oncol*. 2015;25(1):54–64.
5. D'Souza NM, Fang P, Logan J, Yang J, Jiang W, Li J. Combining radiation therapy with immune checkpoint blockade for central nervous system malignancies. *Front Oncol*. 2016;6:212.
6. Formenti SC, Rudqvist NP, Golden E, et al. Radiotherapy induces responses of lung cancer to CTLA-4 blockade. *Nat Med*. 2018;24(12):1845–1851.

7. Reardon DA, Kaley TJ, Dietrich J, et al. Phase II study to evaluate safety and efficacy of MEDI4736 (durvalumab) + radiotherapy in patients with newly diagnosed unmethylated MGMT glioblastoma (new unmeth GBM). *J Clin Oncol.* 2019;37:15(suppl):2032–2032.
8. Ahronian LG, Lewis BC. Using the RCAS-TVA system to model human cancer in mice. *Cold Spring Harb Protoc.* 2014;2014(11):1128–1135.
9. Hambardzumyan D, Amankulor NM, Helmy KY, Becher OJ, Holland EC. Modeling adult gliomas using RCAS/t-va technology. *Transl Oncol.* 2009;2(2):89–95.
10. Chen Z, Feng X, Herting CJ, et al. Cellular and molecular identity of tumor-associated macrophages in glioblastoma. *Cancer Res.* 2017;77(9):2266–2278.
11. Zhu H, Acquaviva J, Ramachandran P, et al. Oncogenic EGFR signaling cooperates with loss of tumor suppressor gene functions in gliomagenesis. *Proc Natl Acad Sci U S A.* 2009;106(8):2712–2716.
12. Holland EC, Hively WP, DePinho RA, Varmus HE. A constitutively active epidermal growth factor receptor cooperates with disruption of G1 cell-cycle arrest pathways to induce glioma-like lesions in mice. *Genes Dev.* 1998;12(23):3675–3685.
13. Mizutani M, Pino PA, Saederup N, Charo IF, Ransohoff RM, Cardona AE. The fractalkine receptor but not CCR2 is present on microglia from embryonic development throughout adulthood. *J Immunol.* 2012;188(1):29–36.
14. Morganti JM, Jopson TD, Liu S, Gupta N, Rosi S. Cranial irradiation alters the brain's microenvironment and permits CCR2+ macrophage infiltration. *PLoS One.* 2014;9(4):e93650.
15. Bloch O, Crane CA, Kaur R, Safaee M, Rutkowski MJ, Parsa AT. Gliomas promote immunosuppression through induction of B7-H1 expression in tumor-associated macrophages. *Clin Cancer Res.* 2013;19(12):3165–3175.
16. Gordon SR, Maute RL, Dulken BW, et al. PD-1 expression by tumour-associated macrophages inhibits phagocytosis and tumour immunity. *Nature.* 2017;545(7655):495–499.
17. Marconi R, Strolin S, Bossi G, Strigari L. A meta-analysis of the abscopal effect in preclinical models: is the biologically effective dose a relevant physical trigger? *PLoS One.* 2017;12(2):e0171559.
18. Ngwa W, Irabor OC, Schoenfeld JD, Hesser J, Demaria S, Formenti SC. Using immunotherapy to boost the abscopal effect. *Nat Rev Cancer.* 2018;18(5):313–322.
19. Rutledge WC, Kong J, Gao J, et al. Tumor-infiltrating lymphocytes in glioblastoma are associated with specific genomic alterations and related to transcriptional class. *Clin Cancer Res.* 2013;19(18):4951–4960.
20. Wang R, Zhou T, Liu W, Zuo L. Molecular mechanism of bystander effects and related abscopal/cohort effects in cancer therapy. *Oncotarget.* 2018;9(26):18637–18647.
21. Verma V, Lin SH. Implications of the bystander and abscopal effects of radiation therapy. *Clin Cancer Res.* 2016;22(19):4763–4765.
22. Huang Y, Lee C, Borgström P, Gjerset RA. Macrophage-mediated bystander effect triggered by tumor cell apoptosis. *Mol Ther.* 2007;15(3):524–533.
23. Hambardzumyan D, Gutmann DH, Kettenmann H. The role of microglia and macrophages in glioma maintenance and progression. *Nat Neurosci.* 2016;19(1):20–27.
24. Charles NA, Holland EC, Gilbertson R, Glass R, Kettenmann H. The brain tumor microenvironment. *Glia.* 2011;59(8):1169–1180.
25. Kerber M, Reiss Y, Wickersheim A, et al. Flt-1 signaling in macrophages promotes glioma growth in vivo. *Cancer Res.* 2008;68(18):7342–7351.
26. Watters JJ, Schartner JM, Badie B. Microglia function in brain tumors. *J Neurosci Res.* 2005;81(3):447–455.
27. Hartley GP, Chow L, Ammons DT, Wheat WH, Dow SW. Programmed cell death ligand 1 (PD-L1) signaling regulates macrophage proliferation and activation. *Cancer Immunol Res.* 2018;6(10):1260–1273.
28. Burrell K, Hill RP, Zadeh G. High-resolution in-vivo analysis of normal brain response to cranial irradiation. *PLoS One.* 2012;7(6):e38366.
29. Kleinovink JW, Marijt KA, Schoonderwoerd MJA, van Hall T, Ossendorp F, Fransen MF. PD-L1 expression on malignant cells is no prerequisite for checkpoint therapy. *Oncoimmunology.* 2017;6(4):e1294299.